

# Vector Portal Pseudo-Goldstone Dark Matter

Ian Chaffey

[ichaf001@ucr.edu](mailto:ichaf001@ucr.edu)

*Department of Physics & Astronomy, University of California, Riverside, CA 92521*

## Abstract

We present a model of pseudo-Goldstone dark matter that interacts through a light vector mediator based on a spontaneously broken  $SU(2)$  dark sector. The dark matter mass is induced by the explicit breaking of the dark  $SU(2)$  symmetry. A residual global  $U(1)$  symmetry prevents dark matter decay. The behavior of this model is studied under the assumption that the observed dark matter relic abundance is due to thermal freeze-out. We consider self-interaction targets for small scale structure anomalies and the possibility of interacting with the Standard model through the vector mediator.

## Contents

<b>1</b>	<b>Introduction</b>	<b>2</b>
<b>2</b>	<b>Symmetry Structure</b>	<b>3</b>
2.1	Lagrangian and Symmetry Breaking Potential . . . . .	3
2.2	Spontaneous Symmetry Breaking . . . . .	4
2.3	Explicit Symmetry Breaking . . . . .	4
2.4	Particle Spectrum . . . . .	5
<b>3</b>	<b>Particles and Mass Spectrum</b>	<b>6</b>
3.1	Gauge Boson Masses . . . . .	6
3.2	vevs and Scalar Boson Masses . . . . .	7
<b>4</b>	<b>Feynman Rules for Dark Sector States</b>	<b>8</b>
<b>5</b>	<b>Relic Abundance</b>	<b>9</b>
<b>6</b>	<b>Self-Interactions</b>	<b>12</b>
<b>7</b>	<b>Portal Interactions</b>	<b>13</b>
<b>8</b>	<b>Conclusion</b>	<b>15</b>

# 1 Introduction

The search for the microscopic description of dark matter is a highly active area of research, situated at the crossroads of particle physics and cosmology. While a massive non-luminous particle is required to resolve the large scale structure of the universe, many of dark matter’s properties remain unknown [1, 2]. A fermionic weakly interacting massive particle (WIMP) has long been a leading candidate for dark matter. As experimental constraints tighten [3–10], dark matter candidates beyond the WIMP paradigm are considered. One such alternative is to consider additional states beyond the dark matter itself, referred to as a “dark” or “hidden” sector [11–16]. Typically, a dark sector consists of a stable dark matter candidate, as well as one or more states that mediate interactions with the visible sector. Often these additional particles are low mass relative to the dark matter. A common framework is the so-called dark photon model where the mediator is a light spin-1 boson. This dark photon may be observable at current and upcoming experiments [14–16]. Such dark sectors with light mediators automatically admit long-range, velocity-dependent interactions that may resolve several small-scale structure anomalies [17].

Spin-0 particles have long been considered as a dark matter candidates. Models of spin-0 dark matter which couple directly to the Standard Model through a Higgs [18–23] or  $Z$ -boson portal [24] have been studied extensively. Dark sector models consisting of spin-0 dark matter and a vector [25, 26] or scalar [27] mediator have been considered. The case of pseudo-Goldstone boson dark matter (PGBDM) offers an interesting alternative to these well understood theories. A massive pseudo-Goldstone boson (PGB) from a softly broken  $U(1)$  symmetry has a vanishing direct detection cross section at zero momentum transfer when scattering off nuclei through a Higgs portal interaction [28, 29] and therefore can circumvent experimental constraints from direct detection experiments. The dark matter in such models remains stable due to a  $\mathbb{Z}_2$  symmetry. These properties have been shown to hold for the fundamental representation of  $SU(N)$  [30], and have been studied in the context of  $B - L$  extensions of the Standard Model [31].

In this manuscript, we consider PGBDM resulting from the spontaneous breaking of a global symmetry group  $SU(2) \times SU(2) \rightarrow SU(2)$ . This symmetry breaking pattern is analogous to chiral symmetry breaking of the flavor symmetry group in which  $SU(2)_L \times SU(2)_R = SU(2)_V \times SU(2)_A$  is broken to the vector subgroup. Here we consider two scalar fields in the fundamental and adjoint representations of a dark sector  $SU(2)$  which, when charged under the vector subgroup, explicitly breaks the axial symmetry. The unbroken  $SU(2)$  subgroup is gauged and spontaneously broken in two steps. First,  $SU(2) \rightarrow U(1)$  at a scale  $f$ . And second,  $U(1) \rightarrow \emptyset$  at a scale  $v \ll f$ . The symmetry structure permits a residual global  $U(1)$  which stabilizes the dark matter, preventing its decay into massless states. The model detailed in this manuscript may also be understood as a phase of the model we present in Ref. [32]. In that work, we developed the first model of spin-1 dark matter with a massive spin-1 mediator which from a non-abelian gauge sector. Small explicit breaking terms give a mass to the pseudo-Goldstone states which respect the residual  $U(1)$  and remain in the spectrum. We consider the phase of the theory in which these pseudo-Goldstones are the lightest particles in the spectrum which respect the residual  $U(1)$ . The resulting spectrum consists of two heavy gauge bosons with mass on the scale  $f$ , a dark photon with mass on the scale  $v$ , the two radial modes responsible for SSB, and the two PGB’s we consider as dark matter candidates. Unlike previous models of PGDM, the global symmetry in this model is not softly broken and thus the direct detection cross section resulting from a Higgs portal interaction does not vanish at zero momentum transfer. Instead, we consider the novel case in which the PGDM interacts with the Standard Model via the dark photon, which couples to the Standard Model hypercharge gauge bosons through kinetic mixing [33, 34]. This scenario is analogous to charged

pion dark matter. While PGDM which couples to the Standard Model through the Higgs portal has been well studied, the case where PGDM couples to the Standard Model via a spin-1 mediator charged under an approximate U(1) symmetry has not been fully explored.

## 2 Symmetry Structure

The scalar sector of our theory consists of an SU(2) doublet  $H^i$  and a triplet  $\Phi = \phi_a T^a$  where  $T^a = \sigma^a/2$  are the generators of SU(2) and  $\sigma^a$  are the Pauli matrices. In the limit of no interactions, the full symmetry group of the dark sector is

$$\text{SU}(2)_\Phi \times \text{SU}(2)_H \times \text{U}(1)_H = \text{SU}(2)_V \times \text{SU}(2)_A \times \text{U}(1)_H \quad (2.1)$$

with the field transformations for the dark sector given by

$$\text{SU}(2)_\Phi : \Phi \rightarrow U_\Phi \Phi U_\Phi^\dagger \quad \text{SU}(2)_H : H \rightarrow U_H H \quad \text{U}(1)_H : H \rightarrow e^{i\theta_H} H \quad (2.2)$$

where  $U_{\Phi,H} = \exp(i\alpha_{\Phi,H}^a T^a)$  is a  $2 \times 2$  special unitary matrix. By analogy to chiral symmetry breaking, we have expressed the full symmetry group in terms of its so called vector and axial subgroups. The vector subgroup corresponds to the transformations where  $U_\Phi = U_H$  while the axial subgroup corresponds to the transformations where  $U_\Phi = U_H^\dagger$ . We gauge the vector subgroup  $\text{SU}(2)_V$ , explicitly breaking  $\text{SU}(2)_A$ . The global  $\text{U}(1)_H$  symmetry corresponds to an accidental ‘‘Higgs number’’ symmetry and behaves similar to Standard Model hypercharge.

### 2.1 Lagrangian and Symmetry Breaking Potential

The most general, renormalizable Lagrangian which respects  $\text{SU}(2)_V \times \text{U}(1)_H$  is:

$$\mathcal{L} = -\frac{1}{4}F_{\mu\nu}^a F^{a\mu\nu} + |DH|^2 + \text{Tr} |\mathcal{D}\Phi|^2 - V(H, \Phi) \quad (2.3)$$

where  $D$  and  $\mathcal{D}$  are the covariant derivatives for SU(2) in the fundamental and adjoint representations respectively. The potential  $V(H, \Phi)$  is responsible for spontaneously breaking  $\text{SU}(2)_V \times \text{U}(1)_H \rightarrow \text{U}(1)_{H'}$  as well as explicitly breaking  $\text{SU}(2)_A$ . The most general renormalizable potential invariant under  $\text{SU}(2)_V \times \text{U}(1)_H$  can be written in the form

$$V = \frac{\lambda}{4!} (2 \text{Tr} \Phi^2 - f_0^2)^2 + \frac{\lambda'}{4!} (2|H|^2 - v_0^2)^2 + \mu H^\dagger \Phi H + \lambda'' |H|^2 \text{Tr} \Phi^2. \quad (2.4)$$

The first term spontaneously breaks  $\text{SU}(2)_\Phi \rightarrow \text{U}(1)_\Phi$ , the second term spontaneously breaks  $\text{SU}(2)_H \rightarrow \emptyset$ , and the trilinear term explicitly breaks  $\text{SU}(2)_A$ . The quartic term proportional to  $\lambda''$  introduces mixing between the doublet and the triplet. Additional quartic terms can all be reduced to the term proportional to  $\lambda''$ . We neglect terms involving the pseudo-conjugate field  $\tilde{H}^i \equiv \epsilon^{ij} H_j^\dagger$  as they violate the  $\text{U}(1)_H$  symmetry which we assume is respected by the Lagrangian. In the following sections we study the symmetry breaking pattern induced by the vacuum expectation values of the scalar fields  $H$  and  $\Phi$ .

## 2.2 Spontaneous Symmetry Breaking

We assume the vacuum expectation values (vevs)

$$\langle \Phi \rangle = fT^3 \qquad \langle H \rangle = \frac{1}{\sqrt{2}} \begin{pmatrix} 0 \\ v \end{pmatrix} \quad (2.5)$$

which break  $SU(2)_\Phi \rightarrow U(1)_\Phi$  and  $SU(2)_H \rightarrow \emptyset$  respectively. All three generators of  $SU(2)_H$  are broken by  $\langle H \rangle$  while the  $SU(2)_\Phi$  generator parallel to  $\langle \Phi \rangle$  remains unbroken. The resulting spectrum of states consists of two massive radial modes and five massless Goldstone bosons: two corresponding to the broken generators of  $SU(2)_\Phi$  and three to the broken generators of  $SU(2)_H$ .

While the  $U(1)_H$  symmetry is spontaneously broken by (2.5), the linear combination

$$T_{H'} = T^3 + \frac{1}{2}T_H, \quad (2.6)$$

where  $T_H$  is the generator of  $U(1)_H$ , remains unbroken. In this representation  $T_{H'} = \mathbb{1}_{2 \times 2}$ . We denote the symmetry generated by  $T_{H'}$  as  $U(1)_{H'}$ . While only the vector subgroup,  $U(1)_V$ , spontaneously broken by  $\langle H \rangle$  is gauged, the associated dark photon's interactions respect  $U(1)_{H'}$  as well. We therefore identify the global *charge* of a dark sector state with respect to this symmetry. This residual symmetry ensures the stability of the lightest charged state.

## 2.3 Explicit Symmetry Breaking

By explicitly breaking the global symmetry group, we can remove all of the massless degrees of freedom from the theory. Our dark sector is constructed to contain two sources of explicit global symmetry breaking:

1. Gauge bosons from the explicit gauging of the subgroup  $SU(2)_V$ .
2. Trilinear mixing between the fundamental scalar  $H$  and adjoint scalar  $\Phi$ .

Gauging  $SU(2)_V$  explicitly breaks  $SU(2)_A$  since the covariant derivatives are constructed to only respect the symmetry of the gauged subgroup. As a result three massless Goldstone modes are eaten by vector bosons, becoming their longitudinal components. The remaining two degrees of freedom become pseudo-Goldstone bosons (PGB) associated with  $SU(2)_A$ . In the absence of explicit symmetry breaking terms in the potential the PGBs are massless at tree level. By introducing a trilinear mixing between  $H$  and  $\Phi$  the PGBs pick up a finite mass proportional to the root of the order of parameter responsible for the explicit breaking  $\mu$ . We can see such a term should be allowed by considering a product of irreducible representations of  $SU(2)$ :

$$\mathbf{2} \otimes \bar{\mathbf{2}} \otimes \mathbf{3} = \mathbf{5} \oplus \mathbf{3} \oplus \mathbf{3} \oplus \mathbf{1}, \quad (2.7)$$

noting that the singlet corresponds to the operator  $H^\dagger \Phi H$ . From (2.2) we can see this operator is clearly invariant under transformations where  $U_H = U_\Phi$ , corresponding to an  $SU(2)_V$  singlet. Since  $SU(2)_A$  is not a proper subgroup of  $SU(2)_\Phi \times SU(2)_H$ , operators of this form which break  $SU(2)_\Phi \times SU(2)_H$  may only be singlets under  $SU(2)_V$  or break the symmetry completely. By removing the massless degrees of freedom we have ensured the lightest stable particle in our dark sector is indeed massive, and thus a viable dark matter candidate.

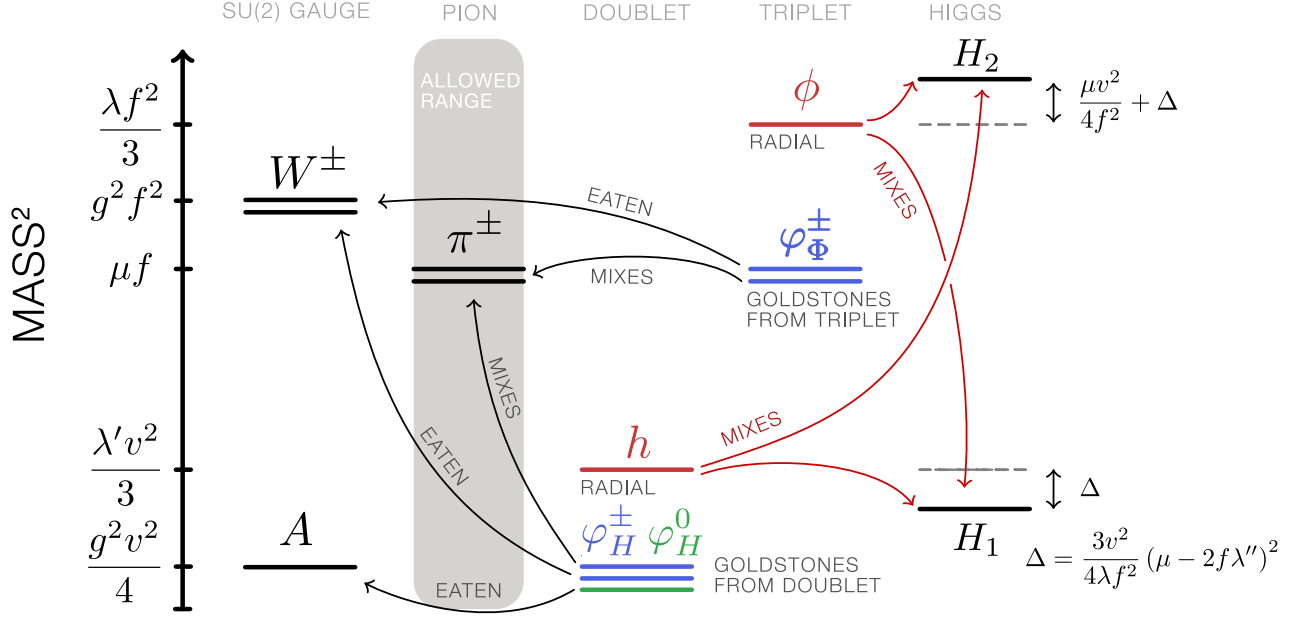


Figure 1: Model spectrum. Mass eigenstates are black lines, charged (neutral) Goldstones are blue (green) lines, radial Higgs modes are red lines. Mixing into mass eigenstates indicated by thin lines.

## 2.4 Particle Spectrum

Our theory yields a rich spectrum of states. After symmetry breaking, the remaining degrees of freedom consist of three massive gauge bosons, the two scalar radial modes, and two massive PGB. We take the limit where

$$\langle \text{Tr } \Phi^2 \rangle = \frac{f^2}{2} \gg \langle |H|^2 \rangle = \frac{v^2}{2} \quad (2.8)$$

setting the mass scale of the gauge boson associated with the broken  $U(1)_V$  subgroup much lower than the gauge bosons corresponding to the other two broken generators. Requiring the mediator to be light and remaining gauge bosons to be heavier than the PGBs amounts to the tuning of a dimensionful renormalizable parameter. The resulting particle content can be summarized as follows:

1. **Dark Matter:** Pseudo-Goldstone bosons  $\pi^\pm$  with mass  $\sim \sqrt{\mu f}$ .
2. **Mediators:** Dark photon  $A$  and light radial mode  $H_1$  with masses  $\sim gv$ , and  $\lambda'v$  respectively.
3. **Heavy modes:**  $W^\pm$  gauge bosons and radial mode  $H_2$  with masses  $\sim gf$  and  $\lambda f$  respectively.

Due to  $U(1)_{H'}$  being unbroken, the lightest charged state remains stable. Since both  $W^\pm$  and  $\pi^\pm$  are charged under  $U(1)_{H'}$ , we assume  $m_\pi < m_W + \min(m_1, m_A) \simeq m_W$ . The opposite case in which  $m_W < m_\pi + \min(m_1, m_A)$  has been studied in Ref. [32]. We label our fields, wherever possible, in analogy to those of the Standard Model in order to highlight their similar roles in the symmetry structure of our theory. We sketch the spectrum in Fig. 1.

### 3 Particles and Mass Spectrum

Following the CCWZ construction [35] we parameterize the scalar fields as rotations of the radial modes by the broken generators

$$\Phi = e^{i\frac{\varphi_\Phi \cdot T}{f}} (\phi + f) T^3 e^{-i\frac{\varphi_\Phi \cdot T}{f}} \quad H = e^{i\frac{\varphi_H \cdot T}{v/2}} \begin{pmatrix} 0 \\ (h+v)/\sqrt{2} \end{pmatrix} \quad (3.1)$$

where we define the broken generators

$$\varphi_\Phi \cdot T = \frac{1}{\sqrt{2}} \varphi_\Phi^+ T^+ + \frac{1}{\sqrt{2}} \varphi_\Phi^- T^- \quad \varphi_H \cdot T = \frac{1}{\sqrt{2}} \varphi_H^+ T^+ + \frac{1}{\sqrt{2}} \varphi_H^- T^- + \varphi_H^0 T^3 \quad (3.2)$$

with  $T^\pm = T^1 \pm iT^2$ . The radial modes  $\phi$  and  $h$  have been expanded about their respective vevs  $f$  and  $v$ . While the scalar fields do mix with the Standard Model Higgs in principle, we consider this coupling to be negligible throughout this work.

#### 3.1 Gauge Boson Masses

The covariant derivatives for the scalar fields are

$$D_\mu H = \partial_\mu H - ig T^a A_\mu^a H \quad \mathcal{D}_\mu = \partial_\mu \Phi - ig A_\mu^a [T^a, \Phi] \quad (3.3)$$

where  $g$  and  $A_\mu^a$  are the  $SU(2)_V$  coupling and gauge field respectively. Evaluating the kinetic terms in the Lagrangian at the vevs gives

$$\mathcal{L} \supset g^2 \left( f^2 + \frac{v^2}{4} \right) W_\mu^+ W_\mu^- + \frac{g^2}{8} v^2 A_\mu A^\mu \quad (3.4)$$

where we have defined the mass eigenstates

$$W^\pm = \frac{1}{\sqrt{2}} (A^1 \mp iA^2) \quad A = A^3 \quad (3.5)$$

such that they are labeled according to their  $U(1)_{H'}$  charges. The gauge boson masses follow directly from (3.4) to be

$$m_W^2 = g^2 \left( f^2 + \frac{v^2}{4} \right) \quad m_A^2 = \frac{g^2 v^2}{4}. \quad (3.6)$$

Even before we diagonalize the potential, the massive psuedo-Goldstone eigenstates can be identified from the kinetic terms of the Lagrangian:

$$|DH|^2 + \text{Tr} |\mathcal{D}\Phi|^2 \supset -g \left( \frac{v}{2} \partial \varphi_H^+ + f \partial \varphi_\Phi^+ \right) W^- + \text{h.c.} - g \frac{v}{2} \partial \varphi_H^0 A. \quad (3.7)$$

A linear combination of  $\varphi_H^\pm$  and  $\varphi_\Phi^\pm$  is eaten by  $W^\pm$  since both  $\langle \Phi \rangle$  and  $\langle H \rangle$  break  $SU(2)_V$  while  $\varphi_H^0$  is only eaten by  $A$  since the  $U(1)_V$  subgroup is only broken  $\langle H \rangle$ . We define the eaten Goldstone  $\varphi_V$  and the orthognal state  $\varphi_A$  as

$$\varphi_V^\pm = \frac{f \varphi_\Phi^\pm + (v/2) \varphi_H^\pm}{\sqrt{f^2 + (v/2)^2}} \quad \varphi_A^\pm = \frac{f \varphi_H^\pm - (v/2) \varphi_\Phi^\pm}{\sqrt{f^2 + (v/2)^2}}. \quad (3.8)$$

$\varphi_A$  is the would-be Goldstone of the spontaneously broken axial symmetry. The Goldstone mode  $\varphi_V^\pm$  is eaten by  $W^\pm$  contributing to it's longitudinal polarization. When one ignores the trilinear term in (2.4), the  $\varphi_A^\pm$  is massless at tree level. However, due to the broken axial symmetry, loops of the gauge bosons induce a radiative mass.

### 3.2 vevs and Scalar Boson Masses

Minimizing the potential (2.4), we find the vevs to be

$$f^2 = f_0^2 + \frac{3v^2}{\lambda} \left( \frac{\mu}{2f} - \lambda'' \right) \quad v^2 = v_0^2 + \frac{3f^2}{\lambda'} \left( \frac{\mu}{f} - \lambda'' \right) . \quad (3.9)$$

The radial modes  $h$  and  $\phi$  mix in this vacuum. In the basis  $(h, \phi)$ , their mass matrix is given by

$$\mathcal{M}_H^2 = \begin{pmatrix} \frac{\lambda' v^2}{3} & \lambda'' v f - \frac{\mu v}{2} \\ \lambda'' v f - \frac{\mu v}{2} & \frac{\lambda f^2}{3} + \frac{\mu v^2}{4f} \end{pmatrix} . \quad (3.10)$$

The eigenvalues of (3.10) are

$$m_{1,2}^2 = \frac{1}{2} \text{Tr} \mathcal{M}_H^2 \mp \left| \frac{(\mathcal{M}_H^2)_{12}}{\sin 2\alpha} \right| \quad (3.11)$$

where  $\alpha$  is the angle that parameterizes the orthogonal transformation  $\mathcal{O}_\alpha$  that diagonalizes (3.10). We define the transformation:

$$\begin{pmatrix} H_1 \\ H_2 \end{pmatrix} = \mathcal{O}_\alpha \begin{pmatrix} h \\ \phi \end{pmatrix} \quad \mathcal{O}_\alpha = \begin{pmatrix} \cos \alpha & \sin \alpha \\ -\sin \alpha & \cos \alpha \end{pmatrix} \quad (3.12)$$

where the mixing angle  $\alpha$  is related to the model parameters by

$$\tan 2\alpha = \frac{\mu v - 2\lambda'' v f}{\lambda f^2/3 + \mu v^2/4f - \lambda' v^2/3} . \quad (3.13)$$

We can expand (3.11) in the limit  $v \ll f$  yielding the approximate eigenvalues

$$m_1^2 = \frac{\lambda' v^2}{3} - \frac{3v^2}{4\lambda f^2} (\mu - 2f\lambda'')^2 + \mathcal{O} \left( \frac{v^4}{f^4} \right) \quad (3.14)$$

$$m_2^2 = \frac{\lambda f^2}{3} + \frac{\mu v^2}{4f} + \frac{3v^2}{4\lambda f^2} (\mu - 2f\lambda'')^2 + \mathcal{O} \left( \frac{v^4}{f^4} \right) . \quad (3.15)$$

In this limit the masses of the radial modes form a hierarchy such that

$$m_1^2 \sim \lambda' v^2 \ll m_2^2 \sim \lambda f^2 . \quad (3.16)$$

The trilinear term in (2.4) causes the Goldstone modes to mix as well. As we did for the radial modes, we expand (2.4) about the vacuum. In the basis  $(\varphi_\Phi^\pm, \varphi_H^\pm)$  the Goldstone mass matrix is,

$$\mathcal{M}_G^2 = \begin{pmatrix} \frac{\mu v^2}{4f} & -\frac{\mu v}{2} \\ -\frac{\mu v}{2} & \mu f \end{pmatrix} . \quad (3.17)$$

It is easy to see that  $\text{Det} \mathcal{M}_G^2 = 0$ , implying the existence of a zero eigenvalue corresponding to the Goldstone eaten by  $W^\pm$ . The other eigenvalue of (3.17) is simply  $\text{Tr} \mathcal{M}_G^2$ . As we did for the radial modes, we diagonalize  $\mathcal{M}_G^2$  with the orthogonal transformation:

$$\begin{pmatrix} G^\pm \\ \pi^\pm \end{pmatrix} = \mathcal{O}_\beta \begin{pmatrix} \varphi_\Phi^\pm \\ \varphi_H^\pm \end{pmatrix} \quad \mathcal{O}_\beta = \begin{pmatrix} \cos \beta & \sin \beta \\ -\sin \beta & \cos \beta \end{pmatrix} \quad (3.18)$$

where  $\pi^\pm$  is a massive PGB and  $G^\pm$  is the masless Goldstone eaten by  $W^\pm$ . The masses of these states are

$$m_G^2 = 0 \qquad m_\pi^2 = \mu f \left( 1 + \frac{\mu v^2}{4f^2} \right). \quad (3.19)$$

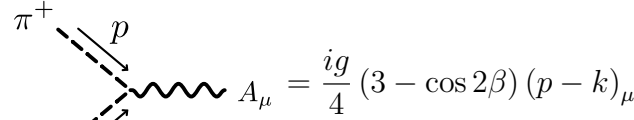
By requiring  $\mathcal{O}_\beta$  diagonalize (3.17), the mixing angle  $\beta$  is found to be

$$\tan \beta = \frac{v}{2f}. \quad (3.20)$$

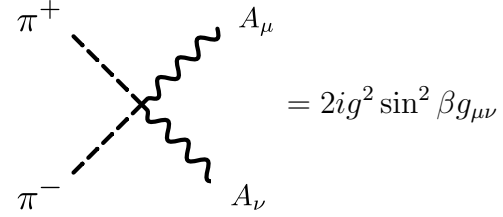
The mass eigenstates defined by (3.18) are identical to the vector and axial states given by (3.8), confirming that  $\text{SU}(2)_A$  is indeed broken by both the gauging of  $\text{SU}(2)_V$  as well as the trilinear term in (2.4). We identify  $\varphi_V^\pm = G^\pm$  and  $\varphi_A^\pm = \pi^\pm$ .

## 4 Feynman Rules for Dark Sector States

We outline the dark sector Feynman rules. Analogous to the interactions between the QCD pion and Standard Model photon, the dark matter interactions with the dark photon are

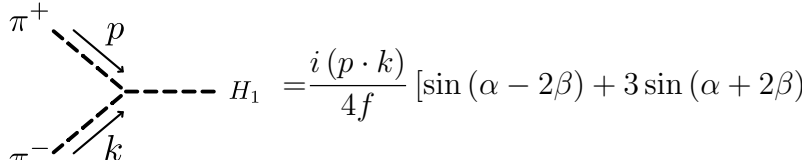


$$A_\mu = \frac{ig}{4} (3 - \cos 2\beta) (p - k)_\mu \quad (4.1)$$

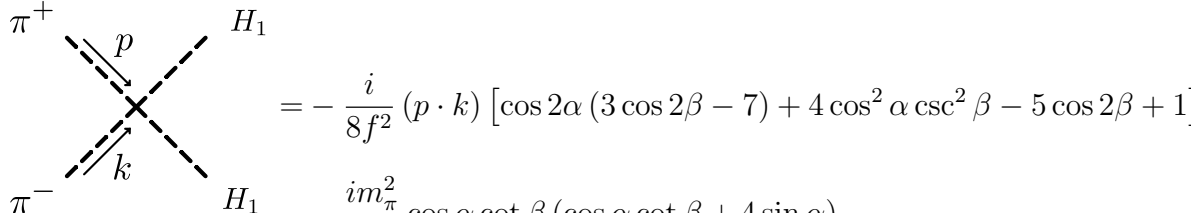


$$= 2ig^2 \sin^2 \beta g_{\mu\nu}. \quad (4.2)$$

The Feynman rules for the dark matter interactions with the light radial mode are



$$H_1 = \frac{i(p \cdot k)}{4f} [\sin(\alpha - 2\beta) + 3 \sin(\alpha + 2\beta)] - \frac{i}{f} (p \cdot k + m_\pi^2) \csc \beta \cos(\alpha - \beta) \quad (4.3)$$



$$H_1 = -\frac{i}{8f^2} (p \cdot k) [\cos 2\alpha (3 \cos 2\beta - 7) + 4 \cos^2 \alpha \csc^2 \beta - 5 \cos 2\beta + 1] - \frac{im_\pi^2}{2f^2} \cos \alpha \cot \beta (\cos \alpha \cot \beta + 4 \sin \alpha). \quad (4.4)$$



Similarly, the dark matter interactions with the heavy radial mode are

$$\begin{aligned}
\begin{array}{c} \pi^+ \\ \swarrow p \\ \searrow k \\ \pi^- \end{array} \quad \begin{array}{c} \text{---} H_2 \end{array} &= \frac{i(p \cdot k)}{4f} [\cos(\alpha - 2\beta) + 3\cos(\alpha + 2\beta)] \\
&+ \frac{i}{f} (p \cdot k + m_\pi^2) \csc \beta \sin(\alpha - \beta)
\end{aligned} \tag{4.5}$$

$$\begin{aligned}
\begin{array}{c} \pi^+ \\ \swarrow p \\ \searrow k \\ \pi^- \end{array} \quad \begin{array}{c} \text{---} H_2 \\ \text{---} H_2 \end{array} &= -\frac{i \sin^2 \beta}{2f^2} (p \cdot k) (\sin^2 \alpha \cot^4 \beta + 4 \cos^2 \alpha) \\
&- \frac{i m_\pi^2}{2f^2} \sin \alpha \cot \beta (\sin \alpha \cot \beta - 4 \cos \alpha) .
\end{aligned} \tag{4.6}$$

The unbroken  $U(1)_{H'}$  allows for the dark matter  $\pi^\pm$  to interact with a  $W^\pm$  of the opposite  $U(1)_{H'}$  charge and a dark photon or radial mode. The Feynman rules are

$$\begin{array}{c} A_\mu \\ \text{wavy} \end{array} \quad \begin{array}{c} \text{---} \pi^+ \end{array} = \frac{g}{2} m_W \sin 2\beta g_{\mu\nu} \tag{4.7}$$

$$\begin{array}{c} W_\nu^- \\ \text{wavy} \end{array} \quad \begin{array}{c} \pi^+ \\ \swarrow q \\ \searrow \end{array} \quad \begin{array}{c} \text{---} H_1 \end{array} = g q_\nu (2 \sin \alpha \sin \beta - \cos \alpha \cos \beta) \tag{4.8}$$

$$\begin{array}{c} \pi^+ \\ \swarrow q \\ \searrow \end{array} \quad \begin{array}{c} \text{---} H_2 \end{array} = g q_\nu (\sin \alpha \cos \beta + 2 \cos \alpha \sin \beta) . \tag{4.9}$$

These interactions mediate the tree-level decay of the  $W^\pm$ .

## 5 Relic Abundance

Dark matter annihilation is dominated by  $s$ -wave processes in the low relative velocity limit. We consider the  $\pi^+\pi^- \rightarrow AA$ ,  $H_1H_1$ , and  $H_2H_2$  channels with all other possibilities being negligible at leading order in  $v/f$ . The diagrams contributing to the  $\pi^+\pi^- \rightarrow AA$  process are shown

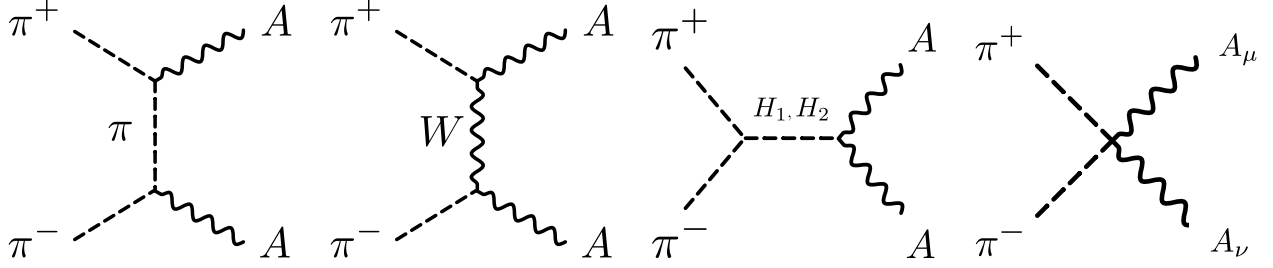


Figure 2: Diagrams contributing to  $\pi^+\pi^- \rightarrow AA$  annihilation. Not shown: crossed ( $u$ -channel) diagrams and annihilation to scalars.

schematically in Fig. 2. To leading order in  $v/f$  the annihilation cross sections are:

$$\sigma v_{AA} = \sigma_0(m_A^2) \left[ \frac{1}{2} + \left( \frac{m_1^2}{4m_A^2} - \frac{m_\pi^2}{2m_W^2} \frac{m_\pi^2 + 5m_W^2}{m_\pi^2 + m_W^2} + X \right)^2 \right] \quad (5.1)$$

$$\sigma v_{H_1 H_1} = \sigma_0(m_1^2) \left[ \frac{m_1^2}{2m_A^2} + \frac{m_\pi^2}{2m_W^2} + \frac{2m_\pi^2}{m_\pi^2 + m_W^2} - X \right]^2 \quad (5.2)$$

$$\sigma v_{H_2 H_2} = \sigma_0(m_2^2) \left[ \frac{m_\pi^2}{4m_W^2} + \frac{YZ}{4m_W^2} - \frac{m_\pi^2}{m_W^2} Y^2 - \frac{m_\pi^4}{m_W^2} \frac{(3+Y)^2}{(m_2^2 - 4m_\pi^2)} + \frac{3m_2^2}{16m_W^2} \frac{(2m_\pi^2 - Z)}{(m_2^2 - 4m_\pi^2)} \right]^2 \quad (5.3)$$

where we have defined the functions

$$\sigma_0(m^2) = \frac{\pi \alpha_X^2}{4m_\pi} \sqrt{1 - \frac{m^2}{m_\pi^2}} \quad (5.4)$$

$$X = \frac{m_\pi^2}{2m_W^2} \frac{m_\pi^2 - 2f^2 \lambda''}{m_2^2 - 4m_\pi^2} \left[ 1 - \frac{2}{m_2^2} (m_\pi^2 - 2f^2 \lambda'') \right] \quad (5.5)$$

$$Y = \left( 1 - \frac{m_\pi^2 - 2f^2 \lambda''}{m_2^2} \right) \quad (5.6)$$

$$Z = (m_\pi^2 - 2f^2 \lambda'') \quad (5.7)$$

as well as the dark fine structure constant

$$\alpha_X = \frac{g^2}{4\pi}. \quad (5.8)$$

We assume that the dark matter relic abundance is due to freeze-out in the early universe. The freeze-out temperature,  $x_f = m_\pi/T_f$ , and relic abundance,  $\Omega h^2$ , are [36]

$$x_f = \ln \left( 0.054 g_*^{-1/2} M_{Pl} m_\pi \langle \sigma v \rangle \right) - \frac{1}{2} \ln^2 \left( 0.054 g_*^{-1/2} M_{Pl} m_\pi \langle \sigma v \rangle \right) \quad (5.9)$$

$$\Omega h^2 = 2 \times 1.07 \times 10^9 \frac{x_f \text{ GeV}^{-1}}{\sqrt{g_*(x_f)} M_{Pl} \langle \sigma v \rangle} \quad (5.10)$$

where we have included an explicit factor of two in order to account for the fact that the dark matter may only annihilate with its anti-particle. The observed dark matter abundance is satisfied when  $\Omega h^2 = 0.12$  [37, 38].

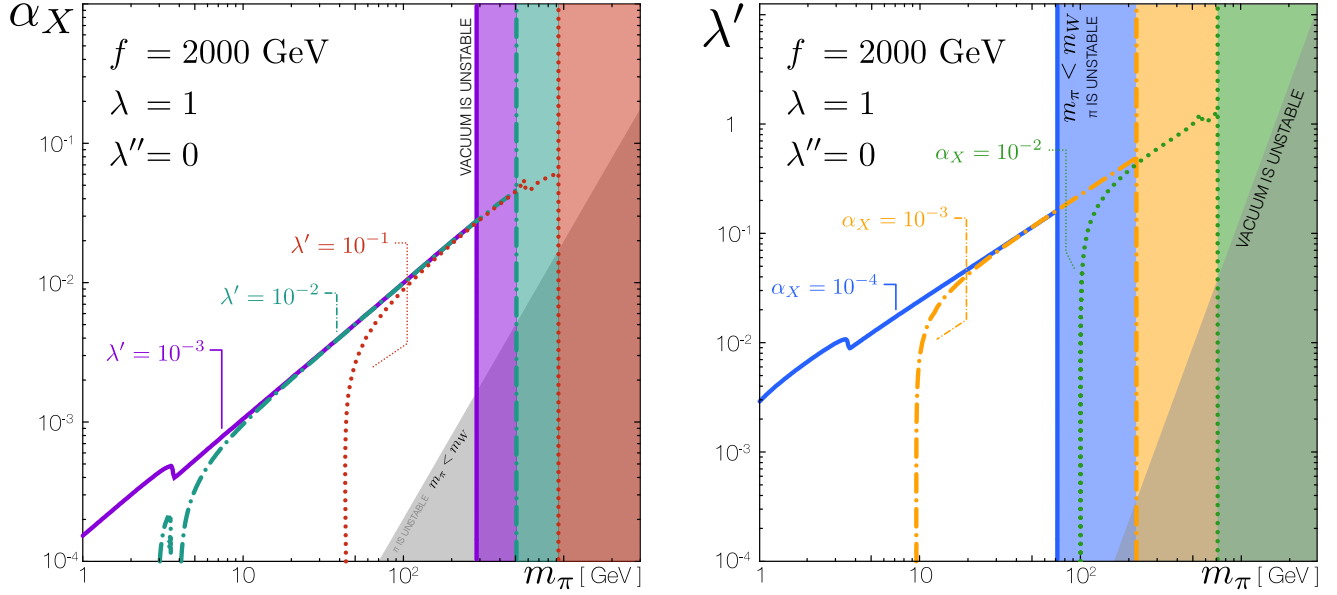


Figure 3: The  $\pi$  relic abundance as a function of the  $\pi$  mass and dark fine structure constant/dark Higgs doublet coupling (Left/Right). The solid (purple/blue), dash-dotted (teal/orange), and dotted (red/green) curves represent when the  $\pi$  saturate the dark matter relic abundance for  $\lambda' = 10^{-1}/\alpha_X = 10^{-2}$ ,  $10^{-2}/10^{-3}$ , and  $10^{-2}/10^{-4}$  respectively. The corresponding solid (purple/blue), dash-dotted (teal/orange), and dotted (red/green) vertical lines bound the regions in which the vacuum/ $\pi$  are unstable. The shaded triangular regions denote where the  $\pi$ /vacuum is unstable.

Fig. 3 shows the values of  $\alpha_X$  (left) and  $\lambda'$  (right) which reproduce the observed relic abundance for a set of benchmark parameters. The curve indicating the observed relic abundance for a given  $\lambda'/\alpha_X$  (Left/Right) becomes vertical when terms in the annihilation cross section independent of  $\alpha_X/\lambda'$  (Left/Right) dominate. This imposes an effective lower bound on  $m_\pi$  for a given set of benchmark parameters.

In this scenario we have implicitly assumed that the dark photon,  $A$ , is in equilibrium with the Standard Model thermal bath. We thus require

$$\Gamma_A \geq H(x_f \cong 20) \quad (5.11)$$

where  $\Gamma_A$  is the dark photon decay width and  $H(x_f)$  is the Hubble rate evaluated at the freeze-out temperature. The resulting constraint on the kinetic mixing parameter  $\varepsilon$  in (7.4) is [13]:

$$\varepsilon^2 \left( \frac{m_A}{10 \text{ MeV}} \right) \gtrsim 10^{-11} \left( \frac{m_\pi}{50 \text{ GeV}} \right)^2. \quad (5.12)$$

This assumption is not strictly necessary for a viable model. One may consider the case in which the dark sector is completely secluded, forming a thermal bath separate from the visible sector with a distinct initial temperature following reheating [39]. The thermal history of dark sectors with mediators has been studied more generally [40–45]. Another possible scenario is that UV dynamics generate an asymmetry in the  $\pi$  abundance [46, 47]. These situations are beyond the scope of this work and we leave them for future study.

## 6 Self-Interactions

Our dark sector automatically yields self-interactions among the  $\pi$ . Dark matter self-interactions were initially identified as a feature of dark sectors [48] and later observed to affect density profiles of dwarf galaxies [49, 50]. More recently, several small-scale structure anomalies have been connected to dark sector models with self-interactions [51–54]. For a detailed review of the full parameter space of dark matter self-interactions see Ref. [17].

The degree to which self-interactions affect dark matter halo densities depends on the scattering rate,  $\sigma v (\rho_{\text{DM}}/m_{\text{DM}})$ . Because the dark matter relative velocity  $v$  and density  $\rho_{\text{DM}}$  are known for the astrophysical systems of interest, the relevant quantity is the ratio of the self-interaction cross section to the dark matter mass,  $\sigma/m_{\text{DM}}$ . Dwarf spheroidal galaxies with low relative velocities ( $v \sim 10$  km/s) suffer from small-scale structure anomalies which may be alleviated in the presence of self-interactions [50, 54, 55]. Galaxy clusters, on the other hand, typically have larger relative velocities ( $v \sim 1500$  km/s) and similarly suffer from small-scale structure anomalies which may also be alleviated by self-interactions. The benchmark values for the ratio of the dark matter self-interaction cross section to its mass are

$$\left(\frac{\sigma}{m_{\text{DM}}}\right)_{\text{dwarf}} \sim 1 \frac{\text{cm}^2}{\text{g}} \qquad \left(\frac{\sigma}{m_{\text{DM}}}\right)_{\text{cluster}} \sim 0.1 \frac{\text{cm}^2}{\text{g}}. \quad (6.1)$$

These seemingly inconsistent target cross sections may be achieved in tandem given the cross section has the appropriate velocity dependence.

The desired velocity dependence is achieved for non-relativistic scattering governed by a Yukawa potential. The dominant contribution to  $\pi^\pm$  self interactions results from the exchange of dark photons,  $A$ , and yields a non-relativistic long-range scattering potential

$$V(r) = \pm \frac{\alpha_\pi}{r} e^{-m_A r} \qquad \alpha_\pi = \frac{\alpha_X}{4} \quad (6.2)$$

where the positive sign corresponds to particle-particle scattering and the negative sign to particle-antiparticle scattering. While the radial modes,  $H_1$  and  $H_2$ , also contribute to self-scattering, the  $\pi^+\pi^-H_1$  vertex, (4.3), is suppressed in the non-relativistic limit when  $v \ll f$ . Therefore we may ignore self-interactions mediated by  $H_1$ . On the other hand,  $m_2 \gg m_A$  implies  $H_2$  mediated self-interactions are sub-dominant compared to interactions mediated by the dark photon,  $A$ , due to the exponential suppression in (6.2) and may be ignored as well.

The benchmark model of SIDM consists of spin-1/2 dark matter with a mass  $\sim 15$  GeV and a spin-1 mediator of mass  $\sim 17$  MeV [55]. The self-interaction potential is assumed to be purely repulsive, implying an asymmetry in the dark matter abundance. Cosmological constraints on dark matter annihilation in early universe typically favor models of asymmetric SIDM, constraining SIDM models with symmetric dark matter abundances to have sub-GeV scale masses [56]. These constraints may be relaxed if we consider cluster scale density profile observations to be satisfied by some other mechanism, allowing for heavier dark matter masses.

Figure 4 compares two symmetric benchmark models in the  $\pi$ SIDM framework to the asymmetric case studied in Ref. [55]. We numerically compute the self-interaction cross section following the methodology of Appendix B of Ref. [32], which is based on the procedure originally presented in Ref. [54]. The solid (blue) curve only satisfies dwarf scale observations and corresponds to dark matter with mass  $m_\pi = 60$  GeV, mediator mass  $m_A = 6$  MeV, and coupling  $\alpha_\pi = 10^{-3}$ . On the other hand, the dashed (orange) curve simultaneously satisfies both dwarf and cluster scale targets, corresponding to dark matter with mass  $m_\pi = 60$  MeV, mediator mass  $m_A = 95$  keV, and coupling

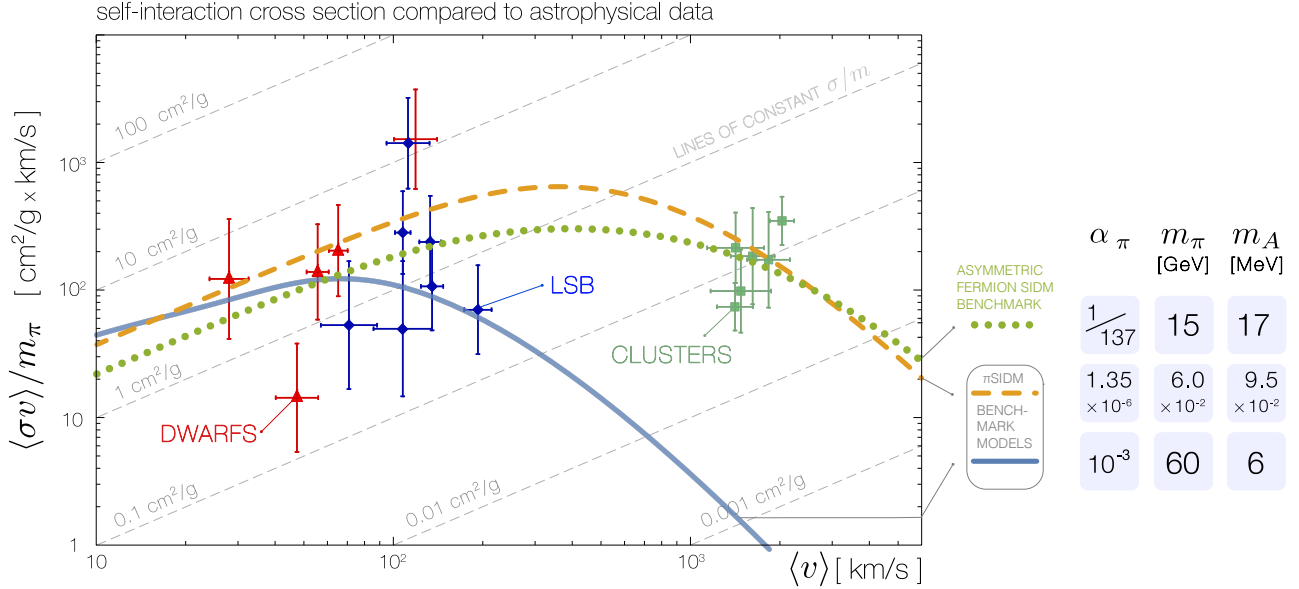


Figure 4: Numerical results for the dark matter self-interaction cross section. The solid/dashed (blue/orange) curves corresponding to benchmarks with symmetric relic abundances, are compared to the dotted (green) curve corresponding to the benchmark model from Ref. [55] with an asymmetric relic abundance. The benchmarks we present are identical to those found for spin-1 dark matter in Ref. [32] with the replacements  $m_W \rightarrow m_\pi$  and  $\alpha_X \rightarrow \alpha_\pi$ .

$\alpha_\pi = 1.35 \times 10^{-6}$ . We compare these benchmarks to the dotted (green) curve which reproduces the model from Ref. [55] with  $m_\pi = 15$  GeV,  $m_A = 17$  MeV, and  $\alpha_\pi = 1/137$ . Because we consider contributions to the self-interaction cross section from both the repulsive and attractive potentials, our benchmarks are not necessarily unique due to the fact that an attractive potential displays resonant behavior [54]. In fact, these are the exact same benchmarks we present in Ref. [32] with  $m_W \rightarrow m_\pi$  and  $\alpha_X \rightarrow \alpha_\pi$ . In the standard freeze out scenario, our benchmark models may be fit to the observed relic abundance by tuning the parameters  $\lambda$ ,  $\lambda'$ , and  $f$ . Ultimately, the cause of dark matter halo density profile observations may be the result of contributions from baryonic feedback [57]. Therefore, we may interpret the data in Figure 4 as upper bounds on the self-interaction cross section.

## 7 Portal Interactions

We consider a renormalizable vector portal interaction between our dark sector to the visible sector. Generally, one may also consider a scalar portal where the dark scalars  $H$  and  $\Phi$  couple to the Standard Model scalar sector through quartic interactions

$$\mathcal{L} \supset \lambda_{H\mathcal{H}} |H|^2 |\mathcal{H}|^2 + \lambda_{\Phi\mathcal{H}} (\text{Tr } \Phi^2) |\mathcal{H}|^2 \quad (7.1)$$

where  $\mathcal{H}$  is the Standard Model Higgs doublet. Models of PGBDM which couple to the visible sector through a Higgs portal have been studied in Refs. [28–31]. In these models, the direct detection signature vanishes at zero momentum transfer as a result of a softly broken global symmetry.<sup>1</sup> Because the axial symmetry group of our model is explicitly broken by a term trilinear in the

<sup>1</sup>In this context, softly broken refers to a symmetry group which is only broken by a mass term.

fields, the direct detection cross section does not contain this feature. Additionally, (7.1) induces mixing between the dark matter,  $\pi$ , and the Standard model Higgs,  $\mathbf{h}$ . We consider the limit where the scalar portal is negligible compared to the vector portal in which the  $\text{SU}(2)_V$  field strength  $F_{\mu\nu} = F_{\mu\nu}^a T^a$  and the adjoint triplet  $\Phi$  may couple to the Standard model hypercharge field strength  $\mathcal{B}^{\mu\nu}$  through the dimension-5 operator

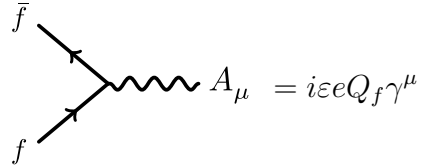
$$\frac{2}{\Lambda} \text{Tr}(\Phi F_{\mu\nu}) \mathcal{B}^{\mu\nu} \quad (7.2)$$

where  $\Lambda$  is the scale of the UV physics which generates this operator. The vev  $\langle \Phi \rangle = f T^3$  induces kinetic mixing between dark photon and visible Standard model photon,

$$\mathcal{L} \supset \frac{\varepsilon}{2 \cos \theta_W} F_{\mu\nu} \mathcal{B}^{\mu\nu} \rightarrow \frac{\varepsilon}{2} F_{\mu\nu} \mathcal{F}^{\mu\nu}, \quad (7.3)$$

where  $\mathcal{F}^{\mu\nu}$  is the visible photon field strength. We do not consider mixing with the Z-boson as its contributions are negligible when the dark photon mass is much below the scale of electroweak symmetry breaking,  $m_A \ll m_Z$ .

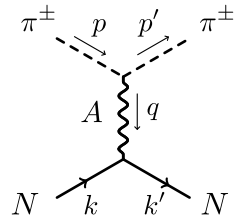
The kinetic mixing given by (7.3) induces a coupling between the dark photon and the Standard Model electromagnetic current. This is consistent with the standard dark photon scenario, and may present signatures at present and future experiments [15, 16]. The Feynman rule for the dark photon,  $A$ , and a fermion,  $f$ , with charge  $Q_f$  is



$$i \varepsilon e Q_f \gamma^\mu. \quad (7.4)$$

For bounds on the coupling  $\varepsilon$  we refer to the reviews [15, 16], as our set up is identical to the standard dark photon.

To demonstrate the bounds on  $\varepsilon$  from direct detection nucleon scattering experiments, we compute the scattering amplitude between dark matter,  $\pi$ , and a charged nucleon,  $N$ ,



$$= \pm \frac{i}{4} \frac{g \varepsilon e Q_N (3 - \cos 2\beta)}{q^2 - m_A^2} \bar{u}(k') (\not{p} + \not{p}') u(k), \quad (7.5)$$

which maps to a spin-independent operator  $\mathcal{O}_1^{(\text{NR})}$  in the non-relativistic limit [58–61]. Matching the notation of Ref. [61], we identify

$$h_3 = \varepsilon e Q_q \quad \text{and} \quad g_4 = \frac{g}{4} (3 - \cos 2\beta). \quad (7.6)$$

We define the effective coupling

$$c_1^N = -2 \frac{g_4 h_3^N}{m_A^2} \quad \Rightarrow \quad c_p \equiv |c_1^N| = \frac{\varepsilon e g}{2 m_A^2} (3 - \cos 2\beta) \simeq \frac{\varepsilon e g}{m_A^2} \quad (7.7)$$

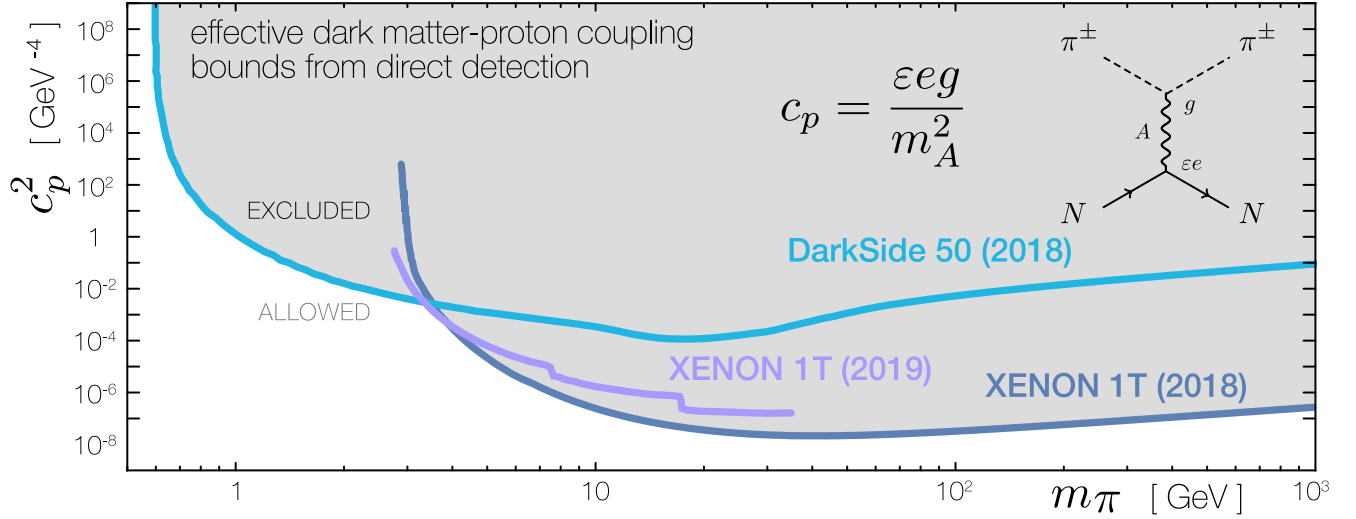


Figure 5: Constraints on the effective dark matter–proton coupling,  $c_p^2$ , from direct detection experiments XENON 1T [62, 63] and DarkSide 50 [64].

where we have assumed the limit  $\tan \beta = v/2f \ll 1$ . Due to the conservation of the electromagnetic charge, the effective coupling  $h_3^N$  for a nucleon,  $N$ , is simply proportional to the charge of the nucleon.

The effective coupling  $c_p$  is constrained by spin-independent dark matter–nucleon scattering from searches such as XENON 1T [62, 63] and DarkSide 50 [64]. We compare the bounds from these searches to the effective coupling  $c_p$  in Fig. 5. For a fixed mediator mass  $m_A$  and dark gauge coupling  $g$ , the spin-independent dark matter–nucleon cross section sets an upper bound on the kinetic mixing parameter,  $\varepsilon$ . While beyond the scope of this study, for values of  $\varepsilon$  so small that the dark sector is effectively decoupled from the visible sector, one may produce thermal histories distinct from the thermal freeze-out scenario [40, 41, 43–45].

## 8 Conclusion

We present a model of pseudo-Goldstone boson dark matter and dark photon mediator. The dark matter mass is finite due to the explicit breaking of the axial subgroup of an  $SU(2) \times SU(2)$  symmetry. Spontaneous symmetry breaking sets the scale of the dark matter and mediator masses, realizing a rich spectrum of states. A residual global  $U(1)$  stabilizes the pseudo-Goldstone states which are assumed to be lightest in the spectrum charged under this symmetry. We find that the PGB states may saturate the observed dark matter relic abundance in the standard thermal freeze-out scenario. For certain benchmark models some small-scale structure anomalies may be resolved by dark matter self-interactions, however the requirement that the dark matter be a thermal relic makes fitting the self-interaction cross section to observations on dwarf galaxy and cluster scales simultaneously difficult. We leave a precise fit of the self-interaction cross section to observed small-scale structure anomalies for future work. We present direct detection bounds on our PGBDM which is assumed to primarily interact with the visible sector through a vector portal. In general a Higgs portal may be considered. However, such interactions introduce further mixing between the PGB states and the radial modes and thus are beyond the scope of this study.

The model presented in this work offers several avenues for further study. One may consider

inelastic scattering off of nucleons, in which a  $\pi^\pm$  up-scatters off of a nucleon producing a  $W^\pm$ . This model may be understood as the phase of the model of spin-1 self-interacting dark matter we present in Ref. [32], where  $m_W > m_\pi$ . Thus, a natural extension of these scenarios is to consider multi-component dark matter in which the observed dark matter abundance consists of a combination of  $\pi^\pm$  and  $W^\pm$ . Such models describe inelastic dark matter which may admit novel phenomenology. Another exciting possibility is to restore the Higgs portal interaction with the visible sector. In this scenario the PGBDM acquires mass mixing with the Standard Model Higgs boson.

## Acknowledgments

We thank Flip Tanedo for insightful discussions. We thank Meghan Neureither and Lemon Neureither-Chaffey for their love and support. We are supported by the DOE grant DE-SC/0008541.

## References

- [1] **Planck** Collaboration, P. A. R. Ade *et al.*, “Planck 2015 results. XIII. Cosmological parameters,” *Astron. Astrophys.* **594** (2016) A13, [arXiv:1502.01589 \[astro-ph.CO\]](#).
- [2] **Planck** Collaboration, N. Aghanim *et al.*, “Planck 2018 results. VI. Cosmological parameters,” [arXiv:1807.06209 \[astro-ph.CO\]](#).
- [3] **PandaX-II** Collaboration, A. Tan *et al.*, “Dark Matter Results from First 98.7 Days of Data from the PandaX-II Experiment,” *Phys. Rev. Lett.* **117** no. 12, (2016) 121303, [arXiv:1607.07400 \[hep-ex\]](#).
- [4] **LUX** Collaboration, D. S. Akerib *et al.*, “Improved Limits on Scattering of Weakly Interacting Massive Particles from Reanalysis of 2013 LUX Data,” *Phys. Rev. Lett.* **116** no. 16, (2016) 161301, [arXiv:1512.03506 \[astro-ph.CO\]](#).
- [5] **LUX** Collaboration, D. S. Akerib *et al.*, “Results from a search for dark matter in the complete LUX exposure,” *Phys. Rev. Lett.* **118** no. 2, (2017) 021303, [arXiv:1608.07648 \[astro-ph.CO\]](#).
- [6] **SuperCDMS** Collaboration, R. Agnese *et al.*, “New Results from the Search for Low-Mass Weakly Interacting Massive Particles with the CDMS Low Ionization Threshold Experiment,” *Phys. Rev. Lett.* **116** no. 7, (2016) 071301, [arXiv:1509.02448 \[astro-ph.CO\]](#).
- [7] D. Hooper, C. Kelso, and F. S. Queiroz, “Stringent and Robust Constraints on the Dark Matter Annihilation Cross Section From the Region of the Galactic Center,” *Astropart. Phys.* **46** (2013) 55–70, [arXiv:1209.3015 \[astro-ph.HE\]](#).
- [8] **Fermi-LAT** Collaboration, M. Ackermann *et al.*, “Searching for Dark Matter Annihilation from Milky Way Dwarf Spheroidal Galaxies with Six Years of Fermi Large Area Telescope Data,” *Phys. Rev. Lett.* **115** no. 23, (2015) 231301, [arXiv:1503.02641 \[astro-ph.HE\]](#).
- [9] L. Bergstrom, T. Bringmann, I. Cholis, D. Hooper, and C. Weniger, “New Limits on Dark Matter Annihilation from AMS Cosmic Ray Positron Data,” *Phys. Rev. Lett.* **111** (2013) 171101, [arXiv:1306.3983 \[astro-ph.HE\]](#).
- [10] M. Cirelli and G. Giesen, “Antiprotons from Dark Matter: Current constraints and future sensitivities,” *JCAP* **1304** (2013) 015, [arXiv:1301.7079 \[hep-ph\]](#).
- [11] M. Pospelov, “Secluded U(1) Below the Weak Scale,” *Phys. Rev.* **D80** (2009) 095002, [arXiv:0811.1030 \[hep-ph\]](#).
- [12] M. Pospelov and A. Ritz, “Astrophysical Signatures of Secluded Dark Matter,” *Phys. Lett.* **B671** (2009) 391–397, [arXiv:0810.1502 \[hep-ph\]](#).
- [13] M. Pospelov, A. Ritz, and M. B. Voloshin, “Secluded WIMP Dark Matter,” *Phys. Lett.* **B662** (2008) 53–61, [arXiv:0711.4866 \[hep-ph\]](#).
- [14] R. Essig *et al.*, “Working Group Report: New Light Weakly Coupled Particles,” in *Proceedings, 2013 Community Summer Study on the Future of U.S. Particle Physics: Snowmass on the Mississippi (CSS2013): Minneapolis, MN, USA, July 29-August 6, 2013*. 2013. [arXiv:1311.0029 \[hep-ph\]](#). <http://www.slac.stanford.edu/econf/C1307292/docs/IntensityFrontier/NewLight-17.pdf>.



- [15] J. Alexander *et al.*, “Dark Sectors 2016 Workshop: Community Report,” 2016. [arXiv:1608.08632 \[hep-ph\]](https://arxiv.org/abs/1608.08632). <http://inspirehep.net/record/1484628/files/arXiv:1608.08632.pdf>.
- [16] M. Battaglieri *et al.*, “Us Cosmic Visions: New Ideas in Dark Matter 2017: Community Report,” in *U.S. Cosmic Visions: New Ideas in Dark Matter College Park, Md, Usa, March 23-25, 2017*. 2017. [arXiv:1707.04591 \[hep-ph\]](https://arxiv.org/abs/1707.04591). <http://lss.fnal.gov/archive/2017/conf/fermilab-conf-17-282-ae-ppd-t.pdf>.
- [17] S. Tulin and H.-B. Yu, “Dark Matter Self-interactions and Small Scale Structure,” *Phys. Rept.* **730** (2018) 1–57, [arXiv:1705.02358 \[hep-ph\]](https://arxiv.org/abs/1705.02358).
- [18] V. Silveira and A. Zee, “Scalar Phantoms,” *Physics Letters B* **161** no. 1, (1985) 136–140. <https://www.sciencedirect.com/science/article/pii/0370269385906240>.
- [19] J. McDonald, “Gauge singlet scalars as cold dark matter,” *Phys. Rev. D* **50** (1994) 3637–3649, [arXiv:hep-ph/0702143](https://arxiv.org/abs/hep-ph/0702143).
- [20] C. Burgess, M. Pospelov, and T. ter Veldhuis, “The Minimal Model of nonbaryonic dark matter: a singlet scalar,” *Nuclear Physics B* **619** no. 1-3, (Dec, 2001) 709–728. [http://dx.doi.org/10.1016/S0550-3213\(01\)00513-2](http://dx.doi.org/10.1016/S0550-3213(01)00513-2).
- [21] T. Cohen, J. Kearney, A. Pierce, and D. Tucker-Smith, “Singlet-doublet dark matter,” *Physical Review D* **85** no. 7, (Apr, 2012) . <http://dx.doi.org/10.1103/PhysRevD.85.075003>.
- [22] E. Ma, “Verifiable radiative seesaw mechanism of neutrino mass and dark matter,” *Physical Review D* **73** no. 7, (Apr, 2006) . <http://dx.doi.org/10.1103/PhysRevD.73.077301>.
- [23] L. L. Honorez, E. Nezri, J. F. Oliver, and M. H. G. Tytgat, “The inert doublet model: an archetype for dark matter,” *Journal of Cosmology and Astroparticle Physics* **2007** no. 02, (Feb, 2007) 028–028. <http://dx.doi.org/10.1088/1475-7516/2007/02/028>.
- [24] M. Escudero, A. Berlin, D. Hooper, and M.-X. Lin, “Toward (finally!) ruling out Z and Higgs mediated dark matter models,” *Journal of Cosmology and Astroparticle Physics* **2016** no. 12, (Dec, 2016) 029–029. <http://dx.doi.org/10.1088/1475-7516/2016/12/029>.
- [25] C. Boehm and P. Fayet, “Scalar dark matter candidates,” *Nuclear Physics B* **683** no. 1-2, (Apr, 2004) 219–263. <http://dx.doi.org/10.1016/j.nuclphysb.2004.01.015>.
- [26] C. Boehm, X. Chu, J.-L. Kuo, and J. Pradler, “Scalar dark matter candidates revisited,” *Phys. Rev. D* **103** no. 7, (2021) 075005, [arXiv:2010.02954 \[hep-ph\]](https://arxiv.org/abs/2010.02954).
- [27] V. Barger, P. Langacker, M. McCaskey, M. Ramsey-Musolf, and G. Shaughnessy, “Complex singlet extension of the standard model,” *Physical Review D* **79** no. 1, (Jan, 2009) . <http://dx.doi.org/10.1103/PhysRevD.79.015018>.
- [28] C. Gross, O. Lebedev, and T. Toma, “Cancellation Mechanism for Dark-Matter–Nucleon Interaction,” *Phys. Rev. Lett.* **119** no. 19, (2017) 191801, [arXiv:1708.02253 \[hep-ph\]](https://arxiv.org/abs/1708.02253).
- [29] J. M. Cline and T. Toma, “Pseudo-Goldstone dark matter confronts cosmic ray and collider anomalies,” [arXiv:1906.02175 \[hep-ph\]](https://arxiv.org/abs/1906.02175).
- [30] D. Karamitros, “Pseudo Nambu-Goldstone Dark Matter: Examples of Vanishing Direct Detection Cross Section,” *Phys. Rev. D* **99** no. 9, (2019) 095036, [arXiv:1901.09751 \[hep-ph\]](https://arxiv.org/abs/1901.09751).
- [31] N. Okada, D. Raut, and Q. Shafi, “Pseudo-Goldstone dark matter in a gauged  $B - L$  extended standard model,” *Phys. Rev. D* **103** no. 5, (2021) 055024, [arXiv:2001.05910 \[hep-ph\]](https://arxiv.org/abs/2001.05910).
- [32] I. Chaffey and P. Tanedo, “Vector Self-Interacting Dark Matter,” [arXiv:1907.10217 \[hep-ph\]](https://arxiv.org/abs/1907.10217).
- [33] B. Holdom, “Two  $U(1)$ ’s and Epsilon Charge Shifts,” *Phys. Lett.* **166B** (1986) 196–198.
- [34] P. Galison and A. Manohar, “Two  $Z$ ’s or not two  $Z$ ’s?,” *Physics Letters B* **136** no. 4, (1984) 279 – 283. <http://www.sciencedirect.com/science/article/pii/0370269384911614>.
- [35] C. G. Callan, S. Coleman, J. Wess, and B. Zumino, “Structure of Phenomenological Lagrangians. II,” *Phys. Rev.* **177** (Jan, 1969) 2247–2250. <https://link.aps.org/doi/10.1103/PhysRev.177.2247>.
- [36] E. W. Kolb and M. S. Turner, “The Early Universe,” *Front. Phys.* **69** (1990) 1–547.
- [37] **Particle Data Group** Collaboration, M. Tanabashi *et al.*, “Review of Particle Physics,” *Phys. Rev. D* **98** no. 3, (2018) 030001.
- [38] G. Steigman, B. Dasgupta, and J. F. Beacom, “Precise Relic WIMP Abundance and Its Impact on Searches for Dark Matter Annihilation,” *Phys. Rev. D* **86** (2012) 023506, [arXiv:1204.3622 \[hep-ph\]](https://arxiv.org/abs/1204.3622).
- [39] J. L. Feng, H. Tu, and H.-B. Yu, “Thermal Relics in Hidden Sectors,” *JCAP* **0810** (2008) 043, [arXiv:0808.2318 \[hep-ph\]](https://arxiv.org/abs/0808.2318).

- [40] X. Chu, T. Hambye, and M. H. G. Tytgat, “The Four Basic Ways of Creating Dark Matter Through a Portal,” *JCAP* **1205** (2012) 034, [arXiv:1112.0493 \[hep-ph\]](#).
- [41] M. Blennow, E. Fernandez-Martínez, and B. Zaldivar, “Freeze-In Through Portals,” *JCAP* **1401** (2014) 003, [arXiv:1309.7348 \[hep-ph\]](#).
- [42] N. Bernal, X. Chu, C. Garcia-Cely, T. Hambye, and B. Zaldivar, “Production Regimes for Self-Interacting Dark Matter,” *JCAP* **1603** no. 03, (2016) 018, [arXiv:1510.08063 \[hep-ph\]](#).
- [43] G. Krnjaic, “Freezing In, Heating Up, and Freezing Out: Predictive Nonthermal Dark Matter and Low-Mass Direct Detection,” *JHEP* **10** (2018) 136, [arXiv:1711.11038 \[hep-ph\]](#).
- [44] J. A. Evans, S. Gori, and J. Shelton, “Looking for the WIMP Next Door,” *JHEP* **02** (2018) 100, [arXiv:1712.03974 \[hep-ph\]](#).
- [45] C. Dvorkin, T. Lin, and K. Schutz, “Making Dark Matter Out of Light: Freeze-In from Plasma Effects,” *Phys. Rev. D* **99** no. 11, (2019) 115009, [arXiv:1902.08623 \[hep-ph\]](#).
- [46] D. E. Kaplan, M. A. Luty, and K. M. Zurek, “Asymmetric Dark Matter,” *Phys. Rev. D* **79** (2009) 115016, [arXiv:0901.4117 \[hep-ph\]](#).
- [47] M. S. Turner and B. J. Carr, “Why Should Baryons and Exotic Relic Particles Have Comparable Densities?,” *Mod. Phys. Lett. A* **2** (1987) 1–7.
- [48] E. D. Carlson, M. E. Machacek, and L. J. Hall, “Self-Interacting Dark Matter,” *Astrophys. J.* **398** (1992) 43–52.
- [49] D. N. Spergel and P. J. Steinhardt, “Observational Evidence for Selfinteracting Cold Dark Matter,” *Phys. Rev. Lett.* **84** (2000) 3760–3763, [arXiv:astro-ph/9909386 \[astro-ph\]](#).
- [50] R. Dave, D. N. Spergel, P. J. Steinhardt, and B. D. Wandelt, “Halo Properties in Cosmological Simulations of Selfinteracting Cold Dark Matter,” *Astrophys. J.* **547** (2001) 574–589, [arXiv:astro-ph/0006218 \[astro-ph\]](#).
- [51] J. L. Feng, M. Kaplinghat, H. Tu, and H.-B. Yu, “Hidden Charged Dark Matter,” *JCAP* **0907** (2009) 004, [arXiv:0905.3039 \[hep-ph\]](#).
- [52] J. L. Feng, M. Kaplinghat, and H.-B. Yu, “Halo Shape and Relic Density Exclusions of Sommerfeld-Enhanced Dark Matter Explanations of Cosmic Ray Excesses,” *Phys. Rev. Lett.* **104** (2010) 151301, [arXiv:0911.0422 \[hep-ph\]](#).
- [53] M. R. Buckley and P. J. Fox, “Dark Matter Self-Interactions and Light Force Carriers,” *Phys. Rev. D* **81** (2010) 083522, [arXiv:0911.3898 \[hep-ph\]](#).
- [54] S. Tulin, H.-B. Yu, and K. M. Zurek, “Beyond Collisionless Dark Matter: Particle Physics Dynamics for Dark Matter Halo Structure,” *Phys. Rev. D* **87** no. 11, (2013) 115007, [arXiv:1302.3898 \[hep-ph\]](#).
- [55] M. Kaplinghat, S. Tulin, and H.-B. Yu, “Dark Matter Halos as Particle Colliders: Unified Solution to Small-Scale Structure Puzzles from Dwarfs to Clusters,” *Phys. Rev. Lett.* **116** no. 4, (2016) 041302, [arXiv:1508.03339 \[astro-ph.CO\]](#).
- [56] R. Huo, M. Kaplinghat, Z. Pan, and H.-B. Yu, “Signatures of Self-Interacting Dark Matter in the Matter Power Spectrum and the Cmb,” *Phys. Lett. B* **783** (2018) 76–81, [arXiv:1709.09717 \[hep-ph\]](#).
- [57] J. S. Bullock and M. Boylan-Kolchin, “Small-Scale Challenges to the  $\Lambda$ CDM Paradigm,” *Ann. Rev. Astron. Astrophys.* **55** (2017) 343–387, [arXiv:1707.04256 \[astro-ph.CO\]](#).
- [58] J. Fan, M. Reece, and L.-T. Wang, “Non-Relativistic Effective Theory of Dark Matter Direct Detection,” *JCAP* **1011** (2010) 042, [arXiv:1008.1591 \[hep-ph\]](#).
- [59] N. Fornengo, P. Panci, and M. Regis, “Long-Range Forces in Direct Dark Matter Searches,” *Phys. Rev. D* **84** (2011) 115002, [arXiv:1108.4661 \[hep-ph\]](#).
- [60] M. Cirelli, E. Del Nobile, and P. Panci, “Tools for Model-Independent Bounds in Direct Dark Matter Searches,” *JCAP* **1310** (2013) 019, [arXiv:1307.5955 \[hep-ph\]](#).
- [61] J. B. Dent, L. M. Krauss, J. L. Newstead, and S. Sabharwal, “General Analysis of Direct Dark Matter Detection: from Microphysics to Observational Signatures,” *Phys. Rev. D* **92** no. 6, (2015) 063515, [arXiv:1505.03117 \[hep-ph\]](#).
- [62] **XENON** Collaboration, E. Aprile *et al.*, “Dark Matter Search Results from a One Ton-Year Exposure of Xenon1T,” *Phys. Rev. Lett.* **121** no. 11, (2018) 111302, [arXiv:1805.12562 \[astro-ph.CO\]](#).
- [63] **XENON** Collaboration, E. Aprile *et al.*, “Light Dark Matter Search with Ionization Signals in XENON1T,” *Phys. Rev. Lett.* **123** no. 25, (2019) 251801, [arXiv:1907.11485 \[hep-ex\]](#).
- [64] **DarkSide** Collaboration, P. Agnes *et al.*, “Darkside-50 532-Day Dark Matter Search with Low-Radioactivity Argon,” *Phys. Rev. D* **98** no. 10, (2018) 102006, [arXiv:1802.07198 \[astro-ph.CO\]](#).